Combined Radar-Radiometer Surface Soil Moisture and Roughness Estimation

Ruzbeh Akbar, *Member*, *IEEE*, Michael H. Cosh, Peggy E. O'Neill, *Fellow*, *IEEE*, Dara Entekhabi, *Fellow*, *IEEE*, Mahta Moghaddam, *Fellow*, *IEEE*

Abstract— **A robust physics-based combined radar-radiometer, or Active-Passive, surface soil moisture and roughness estimation methodology is presented. Soil moisture and roughness retrieval is performed via optimization, i.e., minimization, of a joint objective function which constrains similar resolution radar and radiometer observations simultaneously. A data-driven and noise-dependent regularization term has also been developed to automatically regularize and balance corresponding radar and radiometer contributions to achieve optimal soil moisture retrievals. It is shown that in order to compensate for measurement and observation noise, as well as forward model inaccuracies, in combined radar-radiometer estimation surface roughness can be considered a free parameter. Extensive Monte-Carlo numerical simulations and assessment using field data have been performed to both evaluate the algorithm's performance and to demonstrate soil moisture estimation. Unbiased root mean squared errors (RMSE) range from 0.18 to 0.03 cm3/cm3 for two different land cover types of corn and soybean. In summary, in the context of soil moisture retrieval, the importance of consistent forward emission and scattering development is discussed and presented.**

Index Terms—**Soil Moisture, Radar, Radiometer, Soil Moisture Active-Passive (SMAP)**

I. INTRODUCTION

Knowledge of the amount of surface soil moisture, as a driver behind many of Earth's hydrological and hydroclimatological phenomena, is essential to the science community. Soil moisture dynamics have profound implications on terrestrial water, energy and carbon cycles, as well as evaporation and transpiration at the land-atmosphere boundary. Over continental and regional scales, soil moisture variations also affect weather and climate evolutions. Furthermore, the performance and prediction of current Numerical Weather Prediction (NWP) and global climate models will significantly improve with accurate knowledge of soil moisture, since it is a key initial state variable. In addition, improved flood prediction, drought monitoring, and enhanced agricultural productivity are all made possible with better understanding of soil moisture distributions.

Using current soil moisture measurement technologies, obtaining high resolution and high accuracy global soil moisture predictions meeting stringent science requirements are only possible through merging the strengths of active radar, especially Synthetic Aperture Radar (SAR), with passive radiometer microwave remote sensing techniques. The NASA Soil Moisture Active Passive (SMAP) mission [1], launched in January 2015, sought to address such evolving science requirements and constraints. Prior to the mission's radar ceasing operation, delivering unprecedented high-resolution 9 km global surface soil moisture predictions with a 3-day temporal resolution and volumetric accuracy of 0.04 cm^3/cm^3, or better, was the primary focus of SMAP.

Development of robust Combined Active-Passive (C-AP) retrieval algorithms, applicable to SMAP and other joint radar-radiometer combinations, is of keen interest. In particular, methods that effectively capture the complimentary nature of radar backscatter (σ^0) and radiometer brightness temperature (TB) with respect to variations in land surface conditions for a variety of soil moisture and vegetation regimes have the potential to produce more accurate soil moisture estimates compared to conventional methodologies.

Approximately 2.5 months of global high resolution L-band SMAP radar data were collected prior to instrument failure in July 2015. The existing data are suitable for C-AP algorithm development as well as to further our understanding of the interrelationships between radar backscatter and radiometer emission. Moreover, with an adaptive and robust C-AP algorithm, cross-platform soil moisture estimation may be possible; for example, combining SMAP coarse resolution brightness temperature observations with the European Space Agency's (ESA) Sentinel-1 mission [2] high resolution C-band SAR data are currently under development.

There is a long tradition of soil moisture retrieval using microwave remote sensing; many works have addressed soil moisture observation and estimation from radar-only or radiometer-only perspectives [3][4][5]. Radar and radiometer observations in these studies have shown noticeable sensitivity to changes in surface soil moisture as well as vegetation conditions, followed by attempts to retrieve soil moisture using either radar or radiometer observations. More recently, and

R. Akbar and M. Moghaddam are with the Ming Hsieh Department of Electrical Engineering, University of Southern California, Los Angeles, CA 90089 USA

M. H. Cosh is with the U.S. Department of Agriculture, Agricultural Research Service, Hydrology and Remote Sensing Laboratory, Beltsville, MD 20705 USA

P. O'Neill is with NASA Goddard Space Flight Center, Hydrological Sciences Laboratory, Greenbelt, MD 20771 USA.

R. Akbar and D. Entekhabi are with the Department of Civil and Environmental Engineering, Massachusetts Institute of Technology, Cambridge, MA 02139 USA

within the SMAP mission context, various regression, time-series, and change detection methods have been proposed to combine radar and radiometer observations to estimate soil moisture [6][7][8][9].

The focus of this work is on physics-based and forward-model-centric soil moisture retrieval methods. In comparison to localized regression methods or other empirical approaches [10][11][12], physics-based methods are more broadly applicable, but at times require many model parameters some of which are impractical to measure. The common retrieval target amongst most existing methods is only surface soil moisture. An assumption is typically made about the value of all other model parameters, which can either be derived or inferred from ancillary data sources or localized field campaigns. In the case of SMAP, for example, ancillary knowledge of vegetation water content (VWC) is derived from climatological studies based on Moderate Resolution Imaging Spectroradiometer (MODIS) observations.

In addition to soil moisture and vegetation, surface roughness greatly affects measured radar backscatter and radiometer TB. Typically, both backscatter and emission increase with increasing roughness, but to different levels. Furthermore, knowledge of surface roughness is very limited and difficult to measure at local, regional, or global scales. Typically two approaches are taken to overcome this issue: (a) assuming a land cover dependent value for surface roughness statistics such as in [13][14] for radar-only methods or in [15] for radiometer-only methods. (b) time-series approaches, such that within a short window of time, the amount of surface roughness is assumed constant and a two-step optimization is performed, first for roughness then for soil moisture [16].

More information can be inferred about a given scene from simultaneous use of radar backscatter and radiometer TB than each of them alone. Nominally, radar backscatter observations include two co-polarized (HH and VV) channels, and corresponding radiometer observations include two orthogonal linear polarizations of H and V. Radiometer emission and radar scattering exhibit different and unique sensitivities to the underlying land surface conditions, including soil moisture and surface roughness, and collectively convey synergistic but independent information from the scene under observation. Therefore, within a joint radar-radiometer estimation framework, by taking advantage of this added mutual information between backscatter and emission, it is possible to retrieve additional unknowns. For example, both soil moisture and surface roughness can be assumed to be unknown and retrieved from the joint data set.

Validation of retrieved surface roughness values, however, are generally not possible; thus within the retrieval framework they can be considered as free parameters providing more flexibility for accurate retrieval of soil moisture.

In Section II, a self-regularizing combined active-passive (C-AP) soil moisture estimation framework is presented and effects of forward emission and scattering model ambiguities are discussed. Multi-parameter (soil moisture and roughness) estimation for various measurement and observation noise

scenarios is outlined in Section III and applied to field data in Section IV highlighting improved soil moisture estimation using active and passive observations with the same, or similar, spatial resolutions.

It is important to note that the context of this work focuses on building the foundations of a generalized physics-based and model-driven active-passive retrieval methodology. Therefore, the natural progression is to initially focus on the situation where radar and radiometer measurements are at the same resolution, i.e., tower-mounted or airborne observations. The multi-resolution scenario, such as that of SMAP, where radar and radiometer observations are at different spatial resolutions, is the focus of other on-going, but closely related work and are not presented here.

II. MULTI-PARAMETER ESTIMATION

A. Radar-Radiometer Cost Function Definition

Parameter estimation is performed via minimization of a joint Active and Passive cost function, or objective function, denoted as $L_{ap}(\bar{x})$. Same-resolution radar backscatter and radiometer TB are constrained to each other within the cost function, which generically is written as

$$L_{ap}(\bar{x}) = L_a(\bar{x}) + \gamma \cdot L_p(\bar{x}). \qquad (1)$$

$L_a(\bar{x})$ is the radar, or active, contribution, and $L_p(\bar{x})$ is the radiometer, or passive, contribution. The vector $\bar{x}$ is the vector of unknowns. For the analysis discussed in this section, the unknowns are soil surface permittivity (dielectric constant ϵ_r) and RMS height s [m] scaled by the wavelength k, i.e., $\bar{x} = [\epsilon_r, k \cdot s]$. Note that soil permittivity is a surrogate for soil moisture, and for algorithm development and testing they can be interchanged; similarly for surface roughness s and the scaled, or electromagnetic, roughness, $k \cdot s$.

The individual definitions of $L_a(\bar{x})$ and $L_p(\bar{x})$ are written as

$$L_a(\bar{x}) = \sum_{pp=vv,hh} \left| \frac{\sigma_{pp}^0 - \sigma_{pp}^0(\bar{x})}{k_p} \right|^2 \qquad (2.a)$$

$$L_p(\bar{x}) = \sum_{p=V,H} \left| \frac{TB_p - TB_p(\bar{x})}{\Delta T} \right|^2. \qquad (2.b)$$

Same-resolution active and passive measurements are denoted by σ_{pp}^0 and TB_p, respectively, which include all co-polarized measurements (HH, VV for radar and H- and V-pol for radiometer). The quantities $\sigma_{pp}^0(\bar{x})$ and $TB_p(\bar{x})$ are the respective scattering and emission forward models driven by the unknown vector $\bar{x}$. Other model specific parameters, such as vegetation water content (VWC), surface and canopy physical temperatures, etc., are assumed known and not shown for compactness of form.

Observation noise effects as well as electromagnetic scattering and emission model deficiencies can be detrimental to the ability to properly estimate surface soil moisture, and therefore must be properly accounted for within the joint estimation framework. Here, noise terms are denoted as the

expected measurement noise standard deviations which are k_p for radar and ΔT for radiometer.

Combining $L_a(\bar{x})$ and $L_p(\bar{x})$ from Eqs.2, and rearranging the noise terms, yields

$$L_{ap}(\bar{x}) = \sum_{pp=vv,hh} \left| \frac{\sigma_{pp}^0 - \sigma_{pp}^0(\bar{x})}{k_p} \right|^2 \quad (3.a)$$
$$+ \gamma \sum_{p=V,H} \left| \frac{TB_p - TB_p(\bar{x})}{\Delta T} \right|^2$$

$$L_{ap}(\bar{x}) = \frac{1}{k_p^2} \sum_{pp=vv,hh} \left| \sigma_{pp}^0 - \sigma_{pp}^0(\bar{x}) \right|^2 \quad (3.b)$$
$$+ \gamma \frac{1}{\Delta T^2} \sum_{p=V,H} \left| TB_p - TB_p(\bar{x}) \right|^2$$

$$k_p^2 \cdot L_{ap}(\bar{x}) = \sum_{pp=vv,hh} \left| \sigma_{pp}^0 - \sigma_{pp}^0(\bar{x}) \right|^2 + \gamma \left(\frac{k_p}{\Delta T} \right)^2 \quad (3.c)$$
$$\cdot \sum_{p=V,H} \left| TB_p - TB_p(\bar{x}) \right|^2$$

$$L_{ap}(\bar{x}) = \sum_{pp=vv,hh} \left| \sigma_{pp}^0 - \sigma_{pp}^0(\bar{x}) \right|^2 + \alpha \quad (3.d)$$
$$\cdot \sum_{p=V,H} \left| TB_p - TB_p(\bar{x}) \right|^2$$

Even though individual H- or V-pol radar and radiometer channels may incur different amounts of error, it is assumed that on average and over multiple observations the error standard deviations for each channel are the same. Therefore, k_p and ΔT can be factored out for each summation and regrouped. Furthermore, in Eqs. 3.c, the additional k_p^2 only scales $L_{ap}(\bar{x})$ and can be ignored in the optimization algorithm. This is due to the fact that within any optimization scheme, the goal is to minimize objective functions, and scaling them by a positive scalar values does not change the location of their minima. The form of $L_{ap}(\bar{x})$ as presented in Eqs.3.d captures both radar and radiometer contributions and allows for proper regularization as a function of measurements noise.

The new factor α is given as $\gamma \cdot \left(\frac{k_p}{\Delta T} \right)^2$ and is defined as the square of the ratio of radar to radiometer measurement noise standard deviations multiplied by an additional regularization term γ. The factor γ typically ranges from 10^{-3} to 100 for fine tuning. Selection of an optimum land-cover dependent α parameter will be discussed in detail in later sections.

The effectiveness of the cost function to estimate soil moisture, in the form written in Eq. 3.d, can now be explained: radar and radiometer measurements are tied and constrained to each other but their relative weights are modified based on measurement noise. For added computational stability and flexibility an additional regularization term is also included. Initially, assuming γ to be one ($\gamma = 1$), if the ratio of $\frac{k_p}{\Delta T}$ increases, within $L_{ap}(\bar{x})$ more weight is given to radiometer data. An increase in this ratio is indicative of reduced radiometer noise, or increased radar noise. Conversely, if the $\frac{k_p}{\Delta T}$

ratio decreases, e.g., reduced radar noise or increased radiometer noise, less weight is given to the radiometer data in $L_{ap}(\bar{x})$. Furthermore, by varying γ, as an additional regularization term, optimum balance between σ^0 and TB contributions can be obtained, which results in best retrievals.

Table 1 shows various noise ratio combinations and the resulting minimum and maximum values of α based on varying $\gamma \in [10^{-3}, 100]$. Values of k_p are considered to be as low as 0.5 dB and as high as 0.7 dB [16]. The values of ΔT range from 1.5 K to 3 K. These parameters are also used in the numerical simulations in Section III to demonstrate the performance of this method when retrieving soil moisture.

TABLE 1
ACTIVE-PASSIVE NOISE STANDARD DEVIATION RATIOS
AND REGULARIZATION PARAMETER RANGES

Parameter		Low-Low*	High-High	Low-High	High-Low
$(k_p/\Delta T)^2$		0.11	0.05	0.03	0.22
$\alpha = \gamma \left(\frac{k_p}{\Delta T} \right)^2$	α_{min}	$< 2.2 \cdot 10^{-4}$
	α_{max}	11	5	3	22

* Radar noise standard deviation is mentioned first, then radiometer, i.e. radar/radiometer noise.

Variations of α yield combinations of measurements ranging from radar-only to radiometer-only. Examining the value of $\left(\frac{k_p}{\Delta T} \right)^2$ with respect to changes in the expected radiometer noise ΔT is insightful:

- For the high radiometer noise scenarios, High-High and Low-High, such that $\Delta T \sim 3K$, the ratio $\left(\frac{k_p}{\Delta T} \right)^2$ is small, 0.05 $\left[\frac{dB}{K} \right]^2$ and 0.03 $\left[\frac{dB}{K} \right]^2$, thus automatically reducing the contribution of radiometer measurements and $L_p(\bar{x})$. Under these scenarios, the total value of the cost function is dominated mostly by radar measurements.

- When ΔT is lower, such as in the Low-Low and High-Low scenarios, the value of $\left(\frac{k_p}{\Delta T} \right)^2$ is larger than before, by factor of 3-5, thus naturally adding more weight to radiometer data compared to the previous scenario.

This self-regularizing feature of the cost function greatly improves its robustness with respect to measurement noise when compared to previous methods such as [9] where no distinction was made between the regularization term γ and the noise terms. Furthermore, in the context of SMAP, where TB measurements at the radar resolution do not exist and are produced via a disaggregation scheme [8], ΔT can be interpreted as the uncertainty associated with the disaggregation process and soil moisture estimation performed at the radar resolution.

B. Cost Function Behavior Analysis

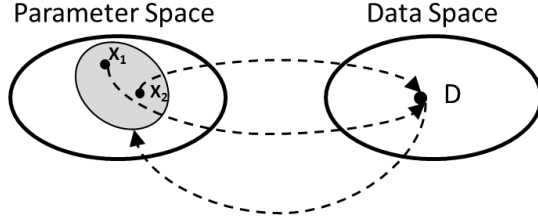In forward model-centric retrieval methods, understanding both model and objective function behavior is key.

Fig. 1: Schematic of parameter and data space non-uniqueness. Both sets of model parameters X_1 and X_2 can generate D. Within the inversion process, especially in the presence of noise, it is unclear what set of parameters caused D, shown as the shaded region.

Forward scattering and emission models can be, and are in this case, non-unique with respect to model parameters and have ambiguities. Specifically, model predictions and outputs based on different combinations of input parameters, i.e., different combinations of soil moisture, roughness, and VWC, can yield similar backscatter or TB output values. This feature greatly complicates the inversion process, especially in the presence of measurement noise. Fig. 1 schematically shows this issue. A single set of model parameters X_1 produces a single observed radar backscatter or radiometer emission value, D. Another set of parameters X_2 can also generate the same value. Ambiguities further arise in the inverse process where, at first glance, it is unclear whether D is due to X_1, X_2 or in the presence of noise, due to a range of possible parameters, shown as the grey shaded area in Fig.1.

In the case of estimating multiple unknown parameters instead of just one, model ambiguities are more severe limiting factors affecting the retrieval performance. In joint radar-radiometer retrievals, such limitations can be mitigated, or even eliminated, by proper utilization of the complimentary information provided by σ^0 and TB measurements.

To highlight the effects of model ambiguity on inversion, and to understand how simultaneously using radar backscatter and radiometer emission measurements can improve soil moisture retrievals, plots of the cost function hyper-planes are examined in Figs. 2, 3 , and 4. For simplification, the hyper-planes are thresholded such that only model predictions within a certain range of true and noise-free test points, D_{true}, are shown. In other words, the range of $\bar{x}$ which makes $|D_{true} - FM(\bar{x})|^2 \leq k_p^2$ (or ΔT^2 in the case of TB) is plotted. The term $FM(\bar{x})$ is either the radar backscatter model or emission model; k_p and ΔT are the expected measurement noise standard deviations, which are squared for consistency in units. They are also taken as the threshold values of the hyper-planes.

Consistent with SMAP baseline radar-only algorithms (L2SM_A), land cover specific radar backscatter datacubes [17][18] are used. These datacubes are pre-computed 3-dimentioal lookup tables generated from analytical scattering models [19] [20]. Co- and cross-pol radar backscatter predictions can be extracted from these datacubes as a function of surface permittivity, surface roughness, and VWC.
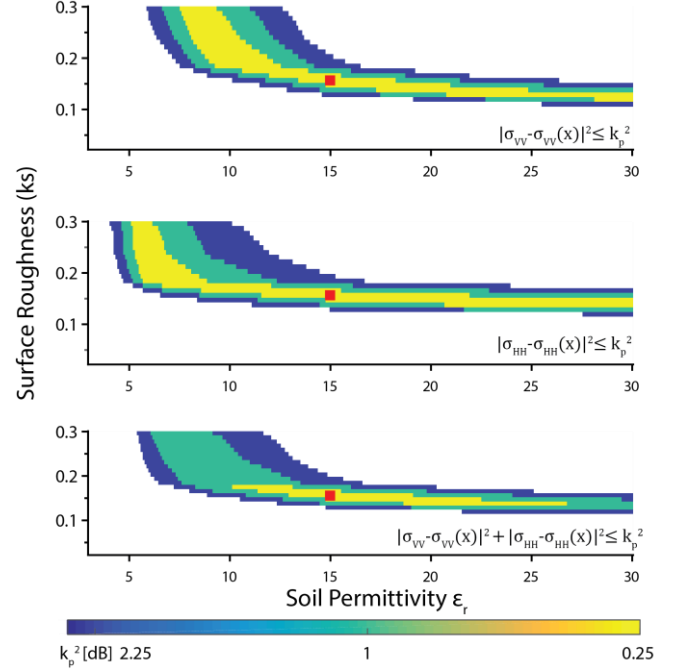

Fig. 2. Radar-only cost function hyper-plane search space. Shaded regions indicate $|\sigma_{true}^0 - \sigma^0(\bar{x})|^2 \leq k_p^2$; $k_p \in \{0.5, 1, 1.5\}$ dB. Red square is the true test point. Top panel VV-only; middle panel HH-only; bottom panel VV and HH

Similarly, the widely accepted tau-omega emission model, or zeroth order solution to the Radiative Transfer equation [4], is used to predict measured brightness temperature as a function of surface permittivity, roughness, VWC, and physical temperature. It is important to note that both models share the same key parameter kernels, i.e., ($\epsilon_r, roughness, \text{VWC}$), although the underlying theoretical development of these models is significantly different. Based on the datacubes's axis discretization, the space of all possible $\bar{x} = [\epsilon_r, k \cdot s]$ values is a 280×30 matrix such that ϵ_r, or soil permittivity, ranges from 3 to 30 with step-length of 0.0968, and root mean squared surface roughness s, scaled by the wavenumber k, is limited between 0 and 0.3 with a step-length of 0.0103.

In Fig. 2, an example hyper-plane for the radar-only cost function, $L_a(\bar{x})$, can be seen. The example here is specific to corn with VWC of 2.5 kg/m². Variations with respect to soil permittivity and surface roughness are initially considered. The VV (top-panel) and HH (middle-panel) responses have been separated since scattering polarization behaviors are different. The shaded regions in Fig. 2 indicate the space of all possible model parameters which produce a model prediction within k_p^2 of the actual measurement. As k_p is gradually reduced from 1.5 dB to 0.5 dB, the effective model parameter search space is reduced, thus showing a gradual convergence towards the true set of model parameters $\bar{x}_{true}$ (Red-squares in Fig. 2).
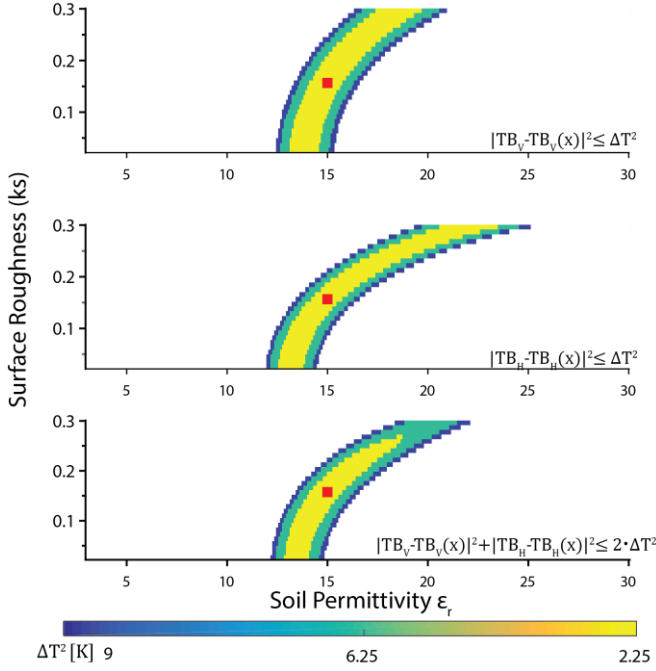
Fig. 3 Radiometer-only cost function hyper-plane search space. Shaded regions indicate $|TB_{true} - TB(\bar{x})|^2 \leq \Delta T^2$; $\Delta T \in \{1.5, 2, 3\}$ K. Red square is the true test point. Top panel TBV-only; middle panel TBH-only; bottom panel TBV and TBH.
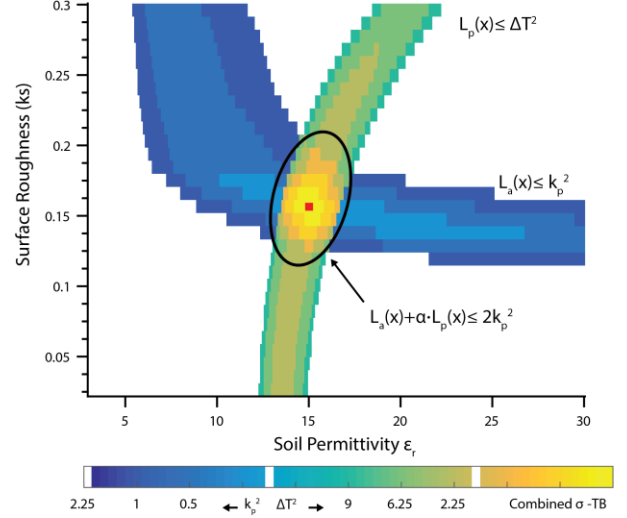

Fig. 4 Overlay of Radar-only ($L_a(\bar{x}) \leq k_p^2$; blue shades) and Radiometer-only ($L_p(\bar{x}) \leq \Delta T^2$; green shades) parameter search spaces. Combined Radar-Radiometer region is the overlap region (yellow shades). The true point is the red square.

Observe that due to the rather ambiguous model response a large range of soil permittivity and roughness combinations are acceptable, from very dry and rough surfaces to wet smooth surfaces. When VV and HH radar backscatter coefficients are simultaneously included, the parameter search space and therefore the ambiguity are effectively reduced (from 25% to 3.5% of the entire range). The range of possible soil permittivity values, however, is still very large ($10 \leq \epsilon_r < 26$). Therefore, it is initially unclear which set of ($\epsilon_r, k \cdot s$) parameter values to select. Consequently, attempting to estimate soil moisture using a single snapshot set of co-pol radar measurements is prone to higher errors.

Figure 3 is analogous to Fig. 2, but for the radiometer case. Again, a large possible search space exits, which spans a wider range of surface roughness compared to soil permittivity. Unlike the radar scenario, the space of possible solutions is limited to a smaller range of soil permittivity values ($12.5 \leq \epsilon_r \leq 17.5$) Inclusion of both TBV and TBH, similar to the radar scenario, reduces the effective search space significantly and the span of possible soil permittivity values is much less than for the case of single polarization TB ($12.5 \leq \epsilon_r \leq 25$).

As seen in Fig. 4, when $L_a(\bar{x})$ and $L_p(\bar{x})$ along with an appropriate regularization term α ($\gamma = 1$), are simultaneously evaluated the parameter search space is significantly reduced. The resulting space is essentially a weighted overlap between radar and radiometer contributions, as indicated by the yellow region in Fig. 4. Since potential target parameters are limited to a smaller region around the true point, more accurate soil moisture retrievals are therefore possible. Furthermore, by varying the contributions of passive data to $L_{ap}(\bar{x})$, via changing α, an optimum weight between $L_a(\bar{x})$ and $L_p(\bar{x})$ can be determined, which further improves the final soil moisture estimates.

In the presence of noise, however, the true set of model parameters may fall outside the search space. Under this condition, a set of parameters $\bar{x}_{opt}$ that minimize $|D - FM(\bar{x})|^2$ must be determined. In Section III, the effects of varying the regularization term γ for various noise scenarios is discussed in detail.

Variations in VWC also increases or decreases the effective model ambiguity and the ability to predict soil moisture. In general, as VWC increases, soil moisture estimation, both from a radar-only and radiometer-only perspective, becomes more erroneous since scattering or emission contributions due to the vegetation gradually dominate the surface response. This feature also affects combined radar-radiometer retrieval approaches. To demonstrate this behavior, the parameter search space based on $L_a(\bar{x}) + \alpha \cdot L_p(\bar{x}) \leq 2 \cdot k_p^2$ for different soil permittivity, roughness and VWC conditions is evaluated and shown in Fig. 5. Here k_p=0.5-1 dB and ΔT=1.5-3K. For a given set of ϵ_r and $k \cdot s$ values, as VWC increases, in general, the parameter search space also expands. However, unlike radar-only or radiometer-only scenarios in Fig. 2 and 3, the span of possible model parameters is much smaller.
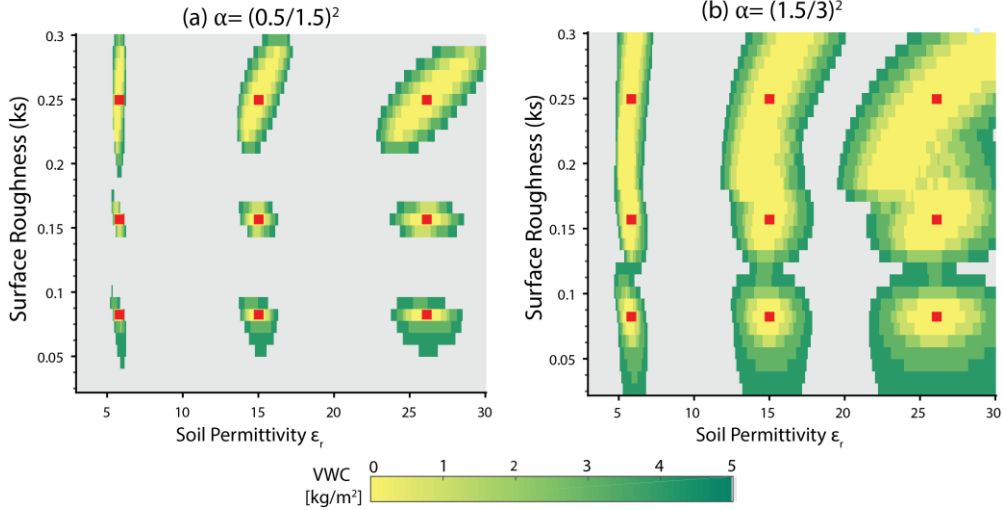
Fig. 5: Combined Radar-Radiometer search spaces gradually increase with increasing VWC, 1 to 5 kg/m². Red Squares indicate different soil ϵ_r and $k \cdot s$ conditions. Left panel shows a low noise scenario ($k_p = 0.5$ dB and $\Delta T = 1.5$ K) and the right panel shows a high noise scenario ($k_p = 1.5$ dB and $\Delta T = 3$ K).

For dry soil conditions and changing VWC values, model ambiguity with respect to variation of surface roughness is larger compared to that due to changes in soil permittivity. This can be observed in the smaller search regions in Fig. 5 (left panel). The increased ambiguity for wetter and rougher surfaces is recognized as signal saturation. More specifically, as the soil moisture content increases, radar backscatter loses sensitivity. Thus, a larger set of possible solutions exists. This is also evident in Fig. 2.

III. SURFACE SOIL MOISTURE AND ROUGHNESS RETRIEVAL

A. Numerical Simulations and Algorithm Performance

To test the performance of the proposed estimation scheme, in the presence of measurement noise, numerical simulations are performed on three distinct land cover types of Corn, Soybean, and Grass. Noisy radar and radiometer measurements are first generated for a large range of soil permittivity, roughness, and VWC conditions as listed in Table II. For both cases, zero mean additive Gaussian noise with standard deviations k_p and ΔT are assumed. Monte-Carlo simulations are then performed with respect to the regularization term α, while soil permittivity and roughness values are retrieved. For each of the noise scenarios listed in Table I, an independent set of numerical simulations is also performed.

Given the compact form of the τ-ω emission model and the fact that no calculations are needed to find σ^0 from the datacubes, it is computationally affordable to use a global optimization scheme such as the Simulated Annealing (SA) method [21]. Optimum values of soil permittivity and roughness $\hat{x} = [\hat{\epsilon}_r, \hat{s}]$, which minimize $L_{ap}(\bar{x})$ in Eq. 3.d are reported as the retrieved parameters. The root mean squared error (RMSE) over the entire range of simulated parameters is

then calculated and reported as a function of the regularization term $\alpha = \gamma \left(\frac{k_p}{\Delta T}\right)^2$. In Fig. 6, plots of RMSE for both soil permittivity and roughness are shown. Panels (a)-(b) are for Corn, (c)-(d) for Grass, and (e)-(f) for Soybean. By varying the regularization term α, through sweeping γ and different $k_p/\Delta T$ ratios, the contributing weights of radar σ^0 and radiometer TB measurements can be changed such that soil moisture estimates with the least retrieval errors are obtained. This feature is clearly seen in the 'dips' (or minima) of the curves in Fig. 6. At the extremes, the optimization process utilizes mostly radar data (α is small) or mostly radiometer data (α is larger). In between, active and passive measurements are weighted such that retrieval errors are minimized.

Based on the noise standard deviation values in Table I, four scenarios for the ratio of radar to radiometer noise, i.e., $k_p/\Delta T$, is assumed: (a) Low noise, where k_p and ΔT are both at their lower bounds, (b) High noise, such that k_p and ΔT are set to their upper bounds, (c) High-Low, and (d) Low-High. The latter two are other noise ratio combinations. As expected, for all land covers, under the high noise scenario, minimum retrieval errors are larger compared to other scenarios, clearly reflecting the impact of measurement noise. Furthermore, for the Low-High case, i.e., low radar but high radiometer noise, minimum retrieval errors are shifted more towards the radar measurements, indicative of a smaller $\left(\frac{k_p}{\Delta T}\right)^2$ ratio and thus discounting TB data. Conversely, for the High-Low scenario, the minimum is shifted more towards radiometer contributions. A summary of Fig. 6 can be see in Table III where the minimum achieved RMSE for soil permittivity and the optimum regularization term for each noise scenario is shown. Similarly, Table IV summarizes RMS errors for surface roughness.

TABLE II
MODEL PARAMETERS FOR NUMERICAL SIMULATIONS

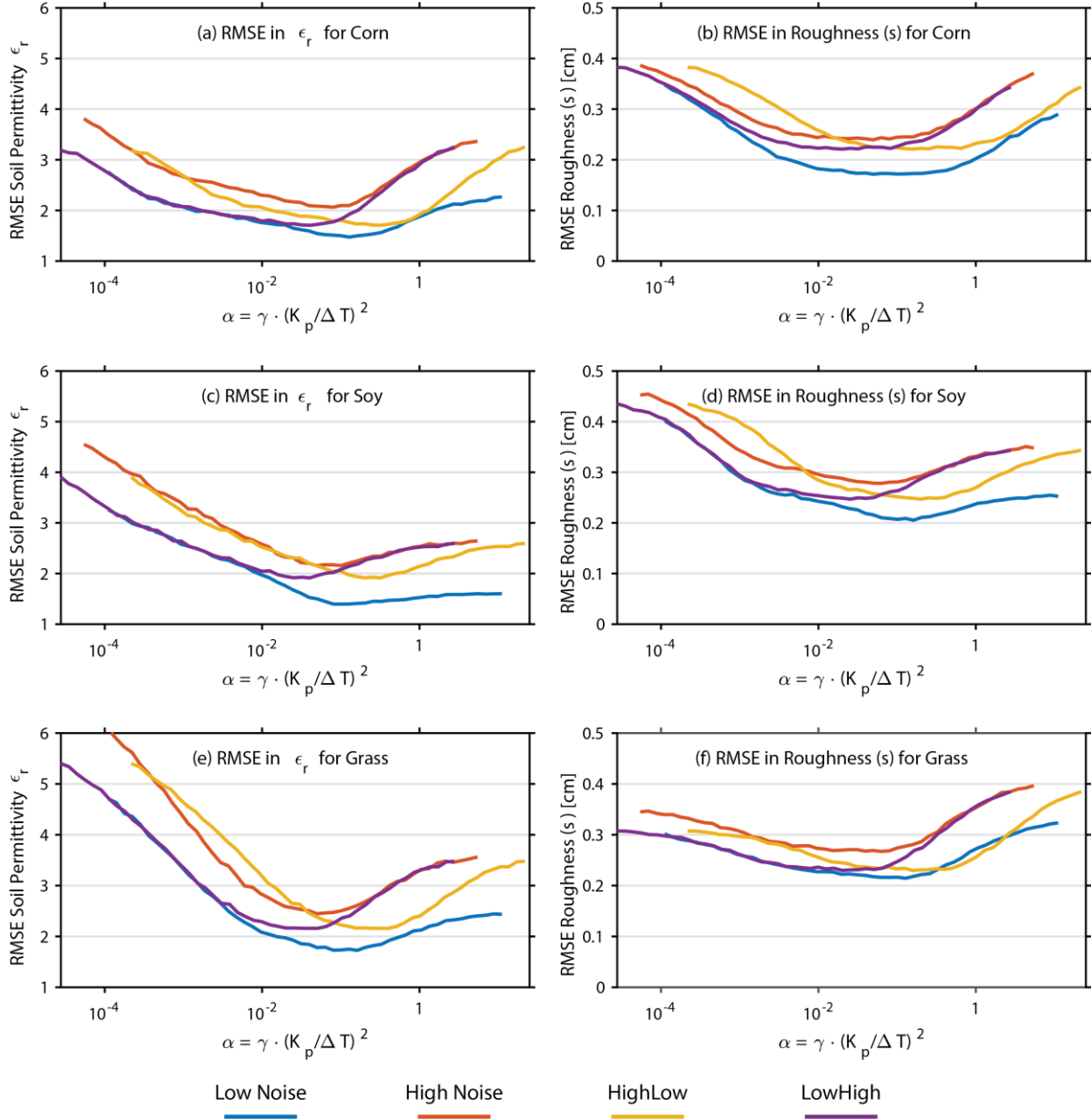| Parameter	Value	Unit
Land Cover Type	Corn, Soybean, Grass	N/A
Soil Permittivity (ϵ_r)	3-30	N/A
Surface Roughness (s)	0.01-1	cm
Vegetation Water Content	0-5	kg/m^2
Radar Noise k_p	0.5-0.7	dB
Radiometer Noise ΔT	1.5-3	K

Fig. 6 Plots of RMSE for Soil Permittivity (left column) and surface roughness (right column). Panels (a)-(b) are Corn, (c)-(d) Soybean, and (e)-(f) Grass. All four noise scenarios listed in Table I are included. Low and High Noise scenarios are when k_P and ΔT are set at their lower bound. High-Low and Low-High are other noise ratio permutations; radar noise, i.e., k_p, is mentioned first.

Across the entire range of soil moisture, roughness, and vegetation parameters, the average RMSE for estimated soil relative permittivity is at most 2.5 and for surface roughness is 0.25 [cm]. Furthermore, observe that the shape and location of error minima for permittivity and roughness are not the same. This is entirely expected since these variables are independent, and their forward model responses and model sensitivities are very different.

Given that independent validation of surface roughness, on any scale, is difficult if not impossible, emphasis is placed on validation and assessment of the retrieved soil permittivity $\hat{\epsilon}_r$. Although the minimum reported errors for surface roughness values, as seen in Figs. 6b-6d and Table IV, are particularly small, roughness is considered a free parameter within the optimization framework.

In practice, sweeping over α or γ terms to find their optimum values, which yield best retrievals, is impractical and time consuming. Therefore, for each land cover type, under the High-High (hh) noise scenario, optimum regularization terms are selected α_{opt}^{hh} and the effect on all other cases is examined. The results are shown in Table V such that for the Low-Low, High-Low, and Low-High cases the actual minimum RMSE for soil permittivity, RMSE at α_{opt}^{hh}, and the incurred relative error by selecting α_{opt}^{hh} are evaluated.

Referring to Tables III and IV, it can be observed that if the optimum value of α is selected from the high noise scenario and applied to all other cases, the resulting relative error is negligible and at most 1.7%. Therefore, a single set of regularization terms can be used for Corn, Soybean, and Grass, namely $\alpha_{opt}^{corn} = 0.08, \alpha_{opt}^{soy} = 0.05, \alpha_{opt}^{grass} = 0.05$. For added flexibility and to fine-tune soil moisture retrievals, γ can be manually varied between 0.9-1.5, or $\alpha \in [0.05\ 0.08]$.

To assess the quality of retrievals, a pair-wise comparison between true test parameters $(\epsilon_{true}, s_{true})$ and their corresponding mean estimates $(\langle\hat{\epsilon}\rangle, \langle\hat{s}\rangle)$ is performed. That is, for discrete pairs of surface roughness and permittivity, covering the ranges as listed in Table II, the mean of the retrieved parameters obtained from Monte-Carlo simulations is compared to the true values. This comparison can be seen in the scatter plot of Fig. 7, where the true and estimated pairs of (ϵ, s) are shown; for a more physically-based interoperation of surface roughness, the values are not scaled by the wavenumber k. The figure shows outcomes of the worst-case scenario, High-High case.

Under perfect retrieval conditions, all mean estimates would align on top of the test case pairs (red-circles). However, in the presence of noise, mean estimates have error, also known as bias. This bias is particularly strong for very rough and very wet surfaces. As observed in Fig. 7, as the surface roughness and soil moisture increase, mean estimates of surface roughness degrades.

Accordingly, errors in predicting soil dielectric constant also increase, however their increase is not as severe as for surface roughness. This is due to selecting optimization results where estimation errors of surface roughness are not minimum, but rather soil permittivity estimation errors are minimum. Furthermore, observe that the biases in surface roughness, except for dry-smooth surfaces, are predominantly negative, whereas for soil permittivity they can be either positive or negative.

TABLE III
MINIMUM SOIL PERMITTIVITY (ϵ_r) RETRIEVAL RMS ERRORS AND OPTIMUM REGULARIZATION TERM VALUES

Land Cover Type	Corn		Soybean		Grass	
Parameter /Noise	Min RMSE	α_{opt}	Min RMSE	α_{opt}	Min RMSE	α_{opt}
High-Low	1.71	0.32	1.91	0.32	2.16	0.32
High-High	2.06	0.08	2.16	0.05	2.45	0.05
Low-High	1.71	0.04	1.91	0.04	2.16	0.04
Low-Low	1.47	0.13	1.40	0.10	1.73	0.16

TABLE IV
MINIMUM SURFACE ROUGHNESS (s) [cm] RETRIEVAL RMSE AND OPTIMUM REGULARIZATION TERM VALUES

Land Cover Type	Corn		Soybean		Grass	
Parameter /Noise	Min RMSE	α_{opt}	Min RMSE	α_{opt}	Min RMSE	α_{opt}
High-Low	0.22	0.16	0.25	0.20	0.23	0.16
High-High	0.24	0.05	0.28	0.06	0.27	0.06
Low-High	0.22	0.02	0.25	0.03	0.23	0.02
Low-Low	0.17	0.05	0.21	0.16	0.21	0.13

TABLE V
WORST CASE RMS ERRORS FOR SOIL RELATIVE PERMITIVITY

Land Cover Type	Parameter	Low-Low	High-Low	Low-High
Corn	Min. RSME	1.47	1.71	1.71
	RMSE at α_{opt}^{hh}	1.50	1.71	1.71
	Relative Error (%)	1.71	< 0.01	< 0.01
Soy	Min. RSME	1.40	1.91	1.91
	RMSE at α_{opt}^{hh}	1.40	1.92	1.92
	Relative Error (%)	< 0.01	0.12	0.12
Grass	Min. RSME	1.73	2.16	2.16
	RMSE at α_{opt}^{hh}	1.73	2.17	2.17
	Relative Error (%)	0.47	0.35	0.35

To capture the error performance of the results in Fig. 7, the RMSE between true and mean estimates of ϵ_r across the whole range of surface roughness are calculated. In the top panel of Fig. 8 this error is shown with a maximum error of about 1.4 for Grass. Components of the Mean Squared Error (MSE), i.e., variance and bias-squared, are also shown in the bottom panel of the figure. For all three land-cover types, as soil permittivity increases, both variance and bias increase. This is due to lack of forward model sensitivity with increasing soil moisture, especially for radar scattering models.
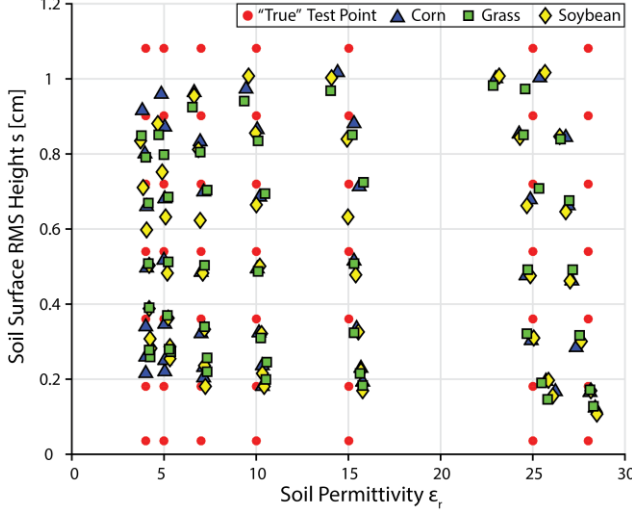
Fig. 7 Scatter plot of pair-wise permittivity-roughness test points and mean estimates for Corn (Blue Triangles), Soybean (Yellow Diamonds), and Grass (Green Squared). Red Circles indicate true test points. Estimation error increases for rougher and wetter soils. Marker offsets from true points indicate the amount of bias due to the optimization.

The MSE for s, similar to Fig. 8, is calculated and shown in Fig. 9. The majority of the error contributing to the total MSE is due to the existing bias, which is also evident in Fig. 7. As mentioned previously, surface roughness estimates are selected from where the estimation error of ϵ_r is minimum; therefore, higher errors for s are expected. Furthermore, given that validation of surface roughness, in practice, is almost impossible, this quantity is viewed as a free parameter allowing the optimization scheme to compensate for measurement and observation noise.

An important metric when evaluating retrieval algorithms is the error performance with respect to changes in VWC. With increasing VWC, vegetation emission and scattering contributions begin to dominate the total measured σ^0 or TB, thus masking surface contributions. This effect was seen in Fig. 5, where the effective search space expanded as VWC increased. To evaluate the upper error bound, for each VWC value the RMS error in ϵ_r across the range of permittivity and roughness is calculated and shown in Fig. 10. Similarly, the error in surface roughness estimation is calculated. Errors in both parameters increase as VWC increases which is commonly observed in many retrieval methods.

B. Soil Moisture Retrieval Using ComRAD Data

The soil moisture retrieval method outlined in the previous section is applied to data obtained from the Combined Radar-Radiometer (ComRAD) tower mounted system [22] [23]. ComRAD is a ground-based simulator of SMAP and includes a quad-pol L-band (1.25 GHz) radar and a dual-pol total-power L-band (1.4 GHz) radiometer. Both instruments share a single parabolic dish antenna with an incident angle of 40°.

During the summer and fall of 2012 (June to October) ComRAD recorded a collection of collocated radar and radiometer measurements overlooking corn and soybean fields.
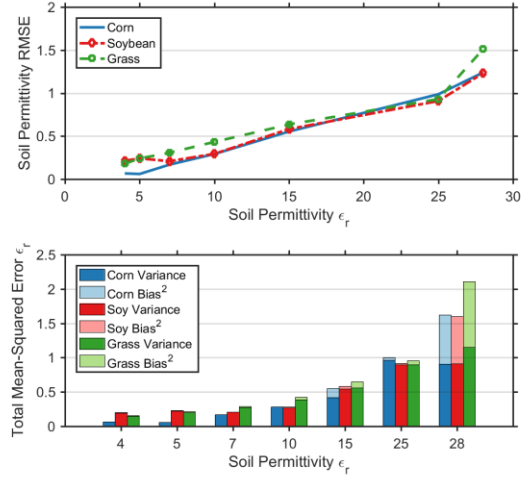

Fig. 8 Worst-case average RMSE for ϵ_r for all three crop types (top panel). Mean Squared Error (MSE) for ϵ_r shown as Variance and Bias² components of the error (bottom panel).
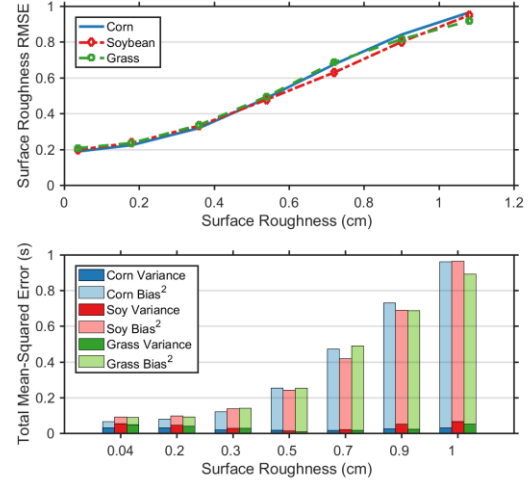

Fig. 9 Worst-case average RMSE for surface roughness s for all three crop types (top panel). Bias contributions to the total MSE dominate the error and increase with increasing s (bottom panel).

These field sites were located at the U.S. Department of Agriculture-Agricultural Research Service (USDA-ARS) Beltsville Agricultural Research Center in Beltsville, MD. Over the duration of the experiment, additional land surface parameters including soil moisture, physical temperature, and VWC were recorded on a regular basis.

Individual radar-only, radiometer-only, and C-AP α_{opt} soil moisture estimates for corn and soybean are shown in the scatter plots of Figs. 13 and 14. Note that for radar-only Corn soil moisture estimates, large portions of the retrievals are capped at approximately 0.44 cm³/cm³. This artifact can be attributed to two underlying reasons and are explained as follows.
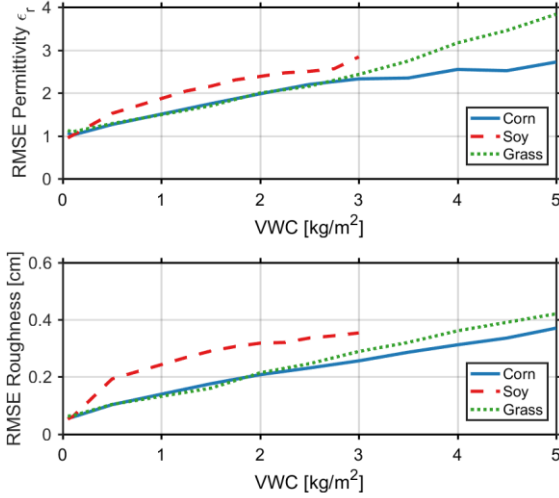
Fig. 10 Average RMSE for ϵ_r increases with increasing VWC for Corn, Soybean and Grass (top panel). Bottom panel shows the RMSE for roughness for the same three vegetation types. Note that the maximum VWC for Soybean is 3 kg/m^2.

Emphasis is placed on validating only retrieved soil moisture. The soil's complex permittivity ϵ_r is first retrieved then converted to soil moisture using the Mironov mixture model [24]. Model and *in situ* Land Surface Parameters (LSP) are summarized in Table VI. This set of parameters has already been used and verified in a previous study [9]. The parameter *b* is generally empirically defined, and in the τ-ω model along with VWC determines the amount of vegetation opacity $\tau = b \cdot VWC$ and emission attenuation $e^{-\tau \cdot \sec \theta_i}$. The single scattering albedo is defined as ω. Radar datacubes for Corn and Soybean, similar to the previous section, are used as the forward scattering models. Soil moisture retrievals will be assessed and compared to the true *in situ* samples based on the following metrics (a) RMSE (b) Correlation coefficients (c) Standard Deviation.

In Fig. 11, as a function of $\alpha = \gamma \left(\frac{k_p}{\Delta T}\right)^2$, the RMSE in estimating soil moisture for both crop types is shown. When α is small, radiometer data are weighted less, thus radar backscatter measurements dominate the cost function. The radar-only RMSE for Corn is 0.22 cm^3/cm^3 and 0.12 cm^3/cm^3 for Soy, both of which are substantially higher than the SMAP acceptance criterion of 0.04 cm^3/cm^3. As α increases, the errors for Corn and Soybean decrease, such that when α is largest, 11.1 [dB/K]^2, radiometer-only inversions yield the smallest errors. This outcome is consistent with previous work [9] where comparisons between forward model predictions and radar measurements showed noticeable error and bias. In short, as α increases, radar induced model-data mismatch effects are reduced and the retrieval error improves. It is important to note here that the form of the objective function only modifies the radiometer-only contributions and their dominance, hence increasing α increases $L_p(\bar{x})$ weights. Alternative objective function forms can be defined such that the regularization term alters radar-only contributions.

TABLE VI
COMRAD IN SITU AND MODEL PARAMETERS

Parameter		Value	Unit
in situ LSP	Soil Moisture	0.03-0.25	cm^3/cm^3
	Corn VWC	0.3-2	kg/m^2
	Soybean VWC	0.3-0.4	kg/m^2
	Surface Roughness	NA	cm
	Clay Fraction	14	%
	Sand Fraction	62	%
	Silt Fraction	24	%
b	Corn	0.01	V-pol
		0.1	H-pol
	Soy	0.01	V-pol
		0.35	H-pol
ω	Corn	0.1	V-pol
		0.01	H-pol
	Soy	0.01	V-pol
		0.01	H-pol
Noise Stn.Dev.	Radar k_p	0.5	dB
	Radiometer ΔT	1.5	K

In the simulation analysis presented in Section III, an optimum regularization parameter was selected for each land cover type of interest. The RMSE at these points are 0.07 cm^3/cm^3, for Corn at $\alpha_{opt}^{corn} = 0.08$, and 0.053 cm^3/cm^3 for Soybean at $\alpha_{opt}^{soy} = 0.05$.

A convenient way to compare the performance of various estimation models with respect to true observations is the use of Taylor diagrams [25], where the three metrics of unbiased RMSE (or Centered RMSE), correlation length, and standard deviation are summarized and presented simultaneously. These statistics for ComRAD retrievals are shown in the Taylor diagrams of Fig. 12. Radar-only (labeled as Radar), radiometer-only (labeled RAD) and combined radar-radiometer at α_{opt} statistics are presented. These values are also summarized in Table VII. Also, a series of other active-passive combinations are plotted to show the progression of statistics as the regularization term changes.

With respect to *in situ* field observations, radiometer-only retrievals have the least unbiased RMSE (0.025 and 0.017 cm^3/cm^3 for Corn and Soy respectively), and comparable standard deviation of 0.03 and 0.04 cm^3/cm^3 for Corn and Soy respectively. Although radar-only estimates show a large correlation with respect to in field measurements, their retrieval RMSE and variations are much larger than radiometer-only outcomes. Statistics calculated at α_{opt} are comparable to radiometer-only values with slightly higher correlations. Both methods, however, do meet the SMAP unbiased RMS error criterion of 0.04 cm^3/cm^3 volumetric soil moisture content.
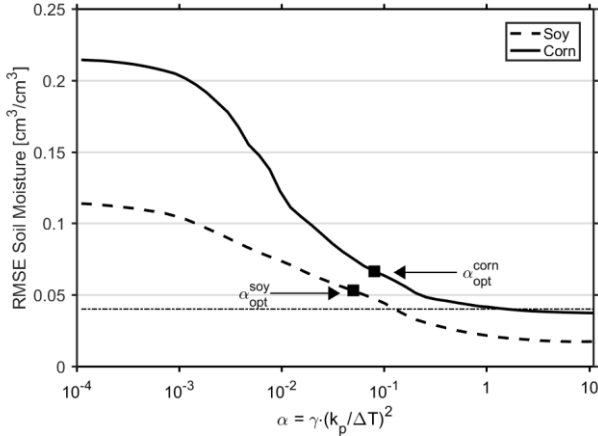
Fig. 11 ComRAD Soil Moisture retrieval RMSE for corn and soybean. Error values at α_{opt} are show by the squares and are 0.07 and 0.053 cm³/cm³ for Corn and Soybean respectively.

First, in a prior study [9], a detailed comparison between ComRAD radar backscatter measurements and the Corn datacube was presented. Using the same available *in situ* soil moisture and Corn VWC information it was observed that the best ComRAD-datacube σ^0 match-up for Corn was achieved when surface roughness was set to about 4.5 [cm]. However, the resulting RMSE between ComRAD σ^0 and model outputs was still significant, e.g., RMSE of 1.2 dB and bias of 0.5 dB for σ^0_{vv}. Similarly, a best-case RMSE of 1.5 dB for Soybean was determined. These discrepancies were attributed to forward model shortcomings and deficiencies, especially when considering the fact that croplands typically have lower levels of roughness.

Second, strict consistency within the active-passive optimization framework has been enforced. That is, both models share the same parameter space as well as the same upper and lower bounds on soil moisture and roughness. More specifically, the radar datacubes' surface roughness has a range of validity up to 5 [cm]. However, in the tau-omega model, surface roughness effects on emission are modeled as an exponential modification to the p-polarized Fresnel Equation r_{0p}, i.e., $r_p = r_{0p}e^{-4(k \cdot s \cdot \cos\theta)^2}$. The upper theoretical limit, at L-band, is typically when $k \cdot s \leq 0.3$ or $s \approx 1$ [cm]. Beyond this value, incoherent surface reflectivity and emission overtake the coherent component, and thus are not modeled properly.

Therefore, knowing that (a) for Corn ComRAD-datacubes σ^0 are closest when surface roughness is about 4.5 [cm] and (b) limiting the optimization's upper bound to 1 [cm], it is expected to see invalid soil moisture retrievals.

To mitigate this artifact, in Fig. 15 Corn radar-only retrievals are regenerated, but with a roughness upper bound of 5 [cm]. A significant improvement in the unbiased RMSE is now observed and the RMSE reduces from 0.113 [cm³/cm³] to 0.041 [cm³/cm³]. Furthermore, individual soil moisture estimates become comparable to outputs for the C-AP α_{opt} case. Under this optimization scenario, models are no longer affected by the parameterization constraints of the pairing forward model.

However, strict active-passive consistency is no longer enforced.

TABLE VII
COMRAD SOIL MOISTURE ESTIMATION STATISTICS

Crop Type	Metrics	Radar-only	Radiometer-only	C-AP at α_{opt}
Corn	ubRMSE	0.113	0.025	0.031
	R^2	0.880	0.805	0.923
	Stn.dev.	0.137	0.042	0.055
Soybean	ubRMSE	0.067	0.017	0.018
	R^2	0.870	0.830	0.900
	Stn.dev.	0.090	0.030	0.040

ubRMSE: Unbiased RMSE; R^2: Correlation Coefficient; Stn.dev.: Standard Deviation; ubRSME and Stn.dev are in [cm³/cm³].

TABLE VIII
COMRAD SURFACE ROUGHNESS ESTIMATES [cm]

Crop Type	Metrics	Radar-only	Radiometer-only	C-AP at α_{opt}
Corn	Mean	0.9	0.95	1.1
	Stn.dev.	0.16	0.34	0.03
Soybean	Mean	0.9	0.8	1.08
	Stn.dev.	0.1	0.3	0.06

The example presented here highlights the importance of consistent forward emission and scattering modeling when performing combined active-passive soil moisture estimation. Since the measured backscatter and TB are dependent on the same set of physical properties of the scene, both models must consistently capture the underlying physical phenomena. Therefore, it is hypothesized that the accuracy of soil moisture retrievals, within an C-AP framework, will significantly increase with a uniform theoretical development of forward models which concurrently predict the amount of emission and scattering, while using a single parameter kernel valid for both physical processes.

IV. CONCLUSION AND DISCUSSION

Through extensive numerical simulations and tests on actual field data it was shown that, in a combined active-passive context with noise dependent self-regularization, soil moisture estimation with errors meeting the SMAP 0.04 [cm³/cm³] volumetric water content accuracy threshold are possible. More specifically, unbiased RMSE for soil moisture using ComRAD data and the proposed objective function, Eq. 3.d, are 0.031 [cm³/cm³] and 0.018 [cm³/cm³] for Corn and Soybean, respectively. Furthermore, by using multiple measurements of difference polarizations (HH, VV, and TB-H and TB-V) the available information space expands and more than one unknown parameter can be retrieved. Specifically, it was shown here that surface soil moisture can be estimated, while at the same time assuming surface roughness to be another unknown, yet free parameter.
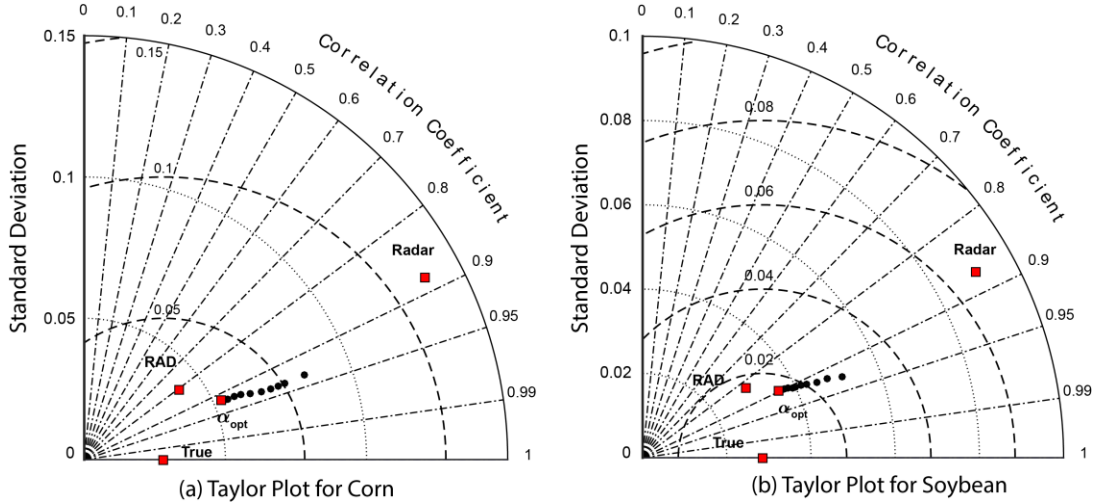
Fig. 12: Taylor diagrams for (a) Corn and (b) Soybean. Radar-only (Radar), Radiometer-only (RAD) and combined radar-radiometer at α_{opt} are shown. Smaller black circles are the statistics for a series of other retrieval efforts prior to α_{opt}. The *in situ* data collected at the same time of ComRAD data acquisitions are marked as "True" with standard deviation of 0.03 and 0.028 cm^3/cm^3 for corn and soybean fields respectively.
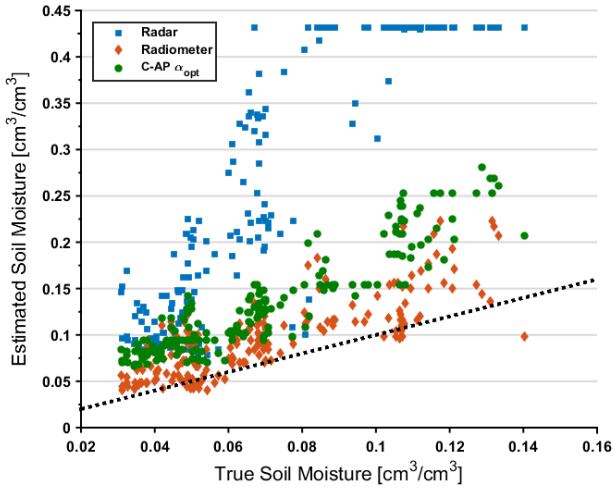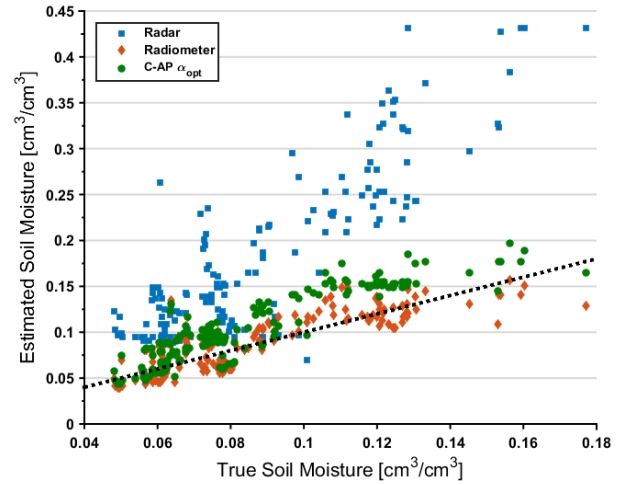

Fig. 13 Radar-only (blue squares), Radiometer-only (red diamonds) and C-AP at α_{opt} (green circles) soil moisture estimates for Corn; respective unbiased RMS errors are 0.113, 0.025, 0.031 [cm^3/cm^3].

Fig. 14 Radar-only (blue squares), Radiometer-only (red diamonds) and C-AP at α_{opt} (green circles) soil moisture estimates for Soybean; respective unbiased RMS errors are 0.067, 0.017, 0.018 [cm^3/cm^3].

One can argue that radiometer-only soil moisture retrievals discussed Section III.B are superior to radar-only or C-AP. A goal of this work, in a broader context, is to develop and present a fully adaptive scheme where it becomes possible to obtain best soil moisture retrievals by fully utilizing the available radar and radiometer information and not rely on a single set of observations or models. If, for a given scenario, radar-only or radiometer-only approaches, within the joint-optimization framework, yield retrievals with least errors, the goal is still achieved.

An alternate application of the proposed objective function is to perform C-AP soil moisture retrieval using high-resolution TB data, derived via disaggregation approaches. Here, ΔT within the regularization term $\gamma \left(\frac{k_p}{\Delta T}\right)^2$ can be interpreted as the expected brightness temperature disaggregation standard deviation error rather than the noise standard deviation for the single resolution scenario.

A key assumption in active-passive soil moisture retrieval at L-band is that both the radar and radiometer observe the same scene, and both forward models share the same unknowns within the optimization. In addition, soils are typically modeled as semi-infinite dielectric slabs with uniform permittivity; thus the C-AP method outputs a single soil moisture value. For environments where there is a meaningful penetration and emission depth difference between radar (1.26 GHz) and radiometer (1.41 GHz), e.g., very dry-sandy soils, the current optimization method is prone to error and outputs cannot be attributed to different depths; the current modeling does not support potential depth differences. Addressing this requires incorporating more accurate soil dielectic, scattering and emission models as well as modifications to the optimization routines.
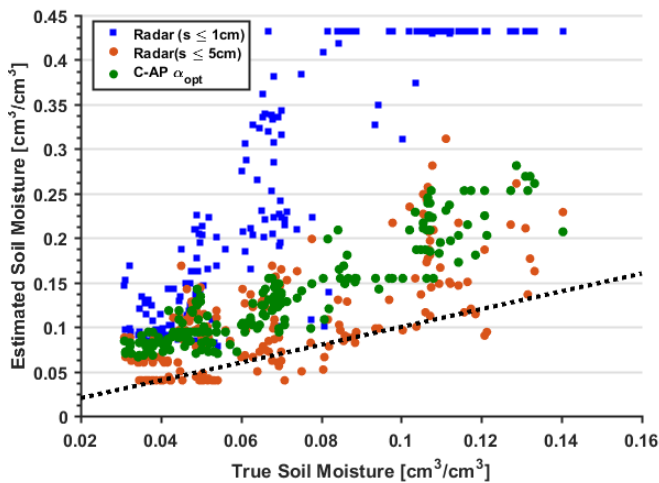
Fig. 15 Radar-only soil moisture estimation for (a) 1 cm surface roughness limit (blue squares) with unbiased RMSE of 0.0113 [cm³/cm³], (b) 5 cm surface roughness limit (red circles) with unbiased RMSE of 0.041 [cm³/cm³], and (c) Radar-only at α_{opt} with unbiased RMSE of 0.031 [cm³/cm³].

For a fully combined active-passive soil moisture estimation technique, development of consistent forward scattering and emission models is also motivated. Models that predict radar backscatter and radiometer emission from a unified theoretical basis can significantly improve soil moisture estimation errors. Within such models, firstly a single parameter kernel is used and secondly emission and scattering responses to changes in vegetation and surface roughness are consistently derived. The effects of model and parameterization inconsistencies were highlighted in Fig. 13, where due to both model-data mismatches and limitation on the bounds of surface roughness, unrealistic soil moisture estimates were produced with a high level of error.

V. REFERENCES

[1] D. Entekhabi, et. al., "The Soil Moisture Active Passive (SMAP) Mission," *Proc. IEEE*, vol. 98, no. 5, pp. 704–716, May 2010.
[2] E. Attema, P. Snoeij, M. Davidson, N. Floury, G. Levrini, B. Rommen, and B. Rosich, "The European GMES Sentinel-1 Radar Mission," in *Geoscience and Remote Sensing Symposium, 2008. IGARSS 2008. IEEE International*, 2008, vol. 1, pp. I–94–I–97.
[3] J. D. Bolten, V. Lakshmi, and E. G. Njoku, "Soil moisture retrieval using the passive/active L- and S-band radar/radiometer," *IEEE Trans. Geosci. Remote Sens.*, vol. 41, no. 12, pp. 2792–2801, Dec. 2003.
[4] T. J. Jackson, "III. Measuring surface soil moisture using passive microwave remote sensing," *Hydrol. Process.*, vol. 7, no. 2, pp. 139–152, Apr. 1993.
[5] E. G. Njoku, W. J. Wilson, S. H. Yueh, S. J. Dinardo, F. K. Li, T. J. Jackson, V. Lakshmi, and J. Bolten, "Observations of soil moisture using a passive and active low-frequency microwave airborne sensor during SGP99," *IEEE Trans. Geosci. Remote Sens.*, vol. 40, no. 12, pp. 2659–2673, Dec. 2002.
[6] M. Piles, D. Entekhabi, and A. Camps, "A Change Detection Algorithm for Retrieving High-Resolution Soil Moisture From SMAP Radar and Radiometer Observations," *IEEE Trans. Geosci. Remote Sens.*, vol. 47, no. 12, pp. 4125–4131, Dec. 2009.
[7] N. N. Das, D. Entekhabi, and E. G. Njoku, "An Algorithm for Merging SMAP Radiometer and Radar Data for High-Resolution Soil-Moisture Retrieval," *IEEE Trans. Geosci. Remote Sens.*, vol. 49, no. 5, pp. 1504–1512, May 2011.
[8] N. N. Das, D. Entekhabi, E. G. Njoku, J. J. C. Shi, J. T. Johnson, and A. Colliander, "Tests of the SMAP Combined Radar and Radiometer Algorithm Using Airborne Field Campaign Observations and Simulated Data," *IEEE Trans. Geosci. Remote Sens.*, vol. 52, no. 4, pp. 2018–2028, Apr. 2014.
[9] R. Akbar and M. Moghaddam, "A Combined Active-Passive Soil Moisture Estimation Algorithm With Adaptive Regularization in Support of SMAP," *IEEE Trans. Geosci. Remote Sens.*, vol. 53, no. 6, pp. 3312–3324, Jun. 2015.
[10] Y. Oh, K. Sarabandi, and F. T. Ulaby, "An empirical model and an inversion technique for radar scattering from bare soil surfaces," *IEEE Trans. Geosci. Remote Sens.*, vol. 30, no. 2, pp. 370–381, Mar. 1992.
[11] P. C. Dubois, J. van Zyl, and T. Engman, "Measuring soil moisture with imaging radars," *IEEE Trans. Geosci. Remote Sens.*, vol. 33, no. 4, pp. 915–926, Jul. 1995.
[12] R. D. de Roo, Y. Du, F. T. Ulaby, and M. C. Dobson, "A semi-empirical backscattering model at L-band and C-band for a soybean canopy with soil moisture inversion," *IEEE Trans. Geosci. Remote Sens.*, vol. 39, no. 4, pp. 864–872, Apr. 2001.
[13] A. Tabatabaeenejad, M. Burgin, X. Duan, and M. Moghaddam, "P-Band Radar Retrieval of Subsurface Soil Moisture Profile as a Second-Order Polynomial: First AirMOSS Results," *IEEE Trans. Geosci. Remote Sens.*, vol. 53, no. 2, pp. 645–658, Feb. 2015.
[14] A. Tabatabaeenejad and M. Moghaddam, "Inversion of Subsurface Properties of Layered Dielectric Structures With Random Slightly Rough Interfaces Using the Method of Simulated Annealing," *IEEE Trans. Geosci. Remote Sens.*, vol. 47, no. 7, pp. 2035–2046, Jul. 2009.
[15] E. G. Njoku and L. Li, "Retrieval of land surface parameters using passive microwave measurements at 6-18 GHz," *IEEE Trans. Geosci. Remote Sens.*, vol. 37, no. 1, pp. 79–93, Jan. 1999.
[16] S. B. Kim, L. Tsang, J. T. Johnson, S. Huang, J. J. van Zyl, and E. G. Njoku, "Soil Moisture Retrieval Using Time-Series Radar Observations Over Bare Surfaces," *IEEE Trans. Geosci. Remote Sens.*, vol. 50, no. 5, pp. 1853–1863, May 2012.
[17] S. Kim, M. Moghaddam, L. Tsang, M. Burgin, X. Xu, and E. G. Njoku, "Models of L-Band Radar Backscattering Coefficients Over Global Terrain for Soil Moisture Retrieval," *IEEE Trans. Geosci. Remote Sens.*, vol. 52, no. 2, pp. 1381–1396, Feb. 2014.
[18] M. Burgin, D. Clewley, R. M. Lucas, and M. Moghaddam, "A Generalized Radar Backscattering Model Based on Wave Theory for Multilayer Multispecies Vegetation," *IEEE Trans. Geosci. Remote Sens.*, vol. 49, no. 12, pp. 4832–4845, Dec. 2011.
[19] S. Huang, L. Tsang, E. G. Njoku, and K. S. Chan, "Backscattering Coefficients, Coherent Reflectivities, and Emissivities of Randomly Rough Soil Surfaces at L-Band for SMAP Applications Based on Numerical Solutions of Maxwell Equations in Three-Dimensional Simulations," *IEEE Trans. Geosci. Remote Sens.*, vol. 48, no. 6, pp. 2557–2568, Jun. 2010.
[20] S. Huang and L. Tsang, "Electromagnetic Scattering of Randomly Rough Soil Surfaces Based on Numerical Solutions of Maxwell Equations in Three-Dimensional Simulations Using a Hybrid UV/PBTG/SMCG Method," *IEEE Trans. Geosci. Remote Sens.*, vol. 50, no. 10, pp. 4025–4035, Oct. 2012.
[21] S. Kirkpatrick, C. D. Gelatt, and M. P. Vecchi, "Optimization by Simulated Annealing," *Science*, vol. 220, no. 4598, pp. 671–680, May 1983.
[22] P. O'Neill, A. Joseph, R. Nelson, M. Cosh, T. Jackson, R. Lang, M. Kurum, and M. Spicknall, "ComRAD active / passive microwave measurement of tree canopies," in *Geoscience and Remote Sensing Symposium, 2007. IGARSS 2007. IEEE International*, 2007, pp. 1420–1423.
[23] P. E. O'Neill, R. H. Lang, M. Kurum, C. Utku, and K. R. Carver, "Multi-Sensor Microwave Soil Moisture Remote Sensing: NASA's Combined Radar/Radiometer (ComRAD) System," in *IEEE MicroRad, 2006*, 2006, pp. 50–54.
[24] V. L. Mironov, L. G. Kosolapova, and S. V. Fomin, "Physically and Mineralogically Based Spectroscopic Dielectric Model for Moist Soils," *IEEE Trans. Geosci. Remote Sens.*, vol. 47, no. 7, pp. 2059–2070, Jul. 2009.

[25] K. E. Taylor, "Summarizing multiple aspects of model performance in a single diagram," *J. Geophys. Res. Atmospheres*, vol. 106, no. D7, pp. 7183–7192, Apr. 2001.

Ruzbeh Akbar (S'05–M'13) received the B.S. degree (Summa Cum Laude) from The George Washington University in 2009 and the M.S. degree from University of Michigan, Ann Arbor, MI, USA in 2011, and the Ph.D. degree from The University of Southern California (USC), Los Angeles CA, USA in 2016. All degrees were in Electrical Engineering. He is currently a Postdoctoral Research Associate at the Massachusetts Institute of Technology (MIT) in Cambridge, MA, USA. His Research interests include terrestrial remote sensing, electromagnetic theory, and hydrology. He was the recipient of the NASA Earth and Space Science fellowship (NESSF) between 2010-2014.

Michael H. Cosh received the Ph.D. degree from Cornell University, Ithaca, NY, USA, in 2002. He is a Research Hydrologist with the U.S. Department of Agriculture, Agricultural Research Service, Hydrology and Remote Sensing Laboratory, Beltsville, MD, USA. His research involves the monitoring of soil moisture from both in situ resources and satellite products. Currently, he is serving as the Acting Research Leader for the Hydrology and Remote Sensing Laboratory, which includes 12 scientists working in areas of soil moisture remote sensing, evapotranspiration, and water quality. Dr. Cosh served as the Chairperson of both the Remote Sensing Technical Committee and the Large Scale Field Experiments Technical Committee for the American Geophysical Union.

Peggy E. O'Neill (F'16) received the B.S. degree (summa cum laude with University Honors) in geography from Northern Illinois University, DeKalb, IL, USA, in 1976 and the M.A. degree in geography from the University of California, Santa Barbara, CA, USA, in 1979. She has done postgraduate work in civil and environmental engineering through Cornell University. She is currently the SMAP Deputy Project Scientist. Since 1980, she has been a Physical Scientist with the Hydrological Sciences Laboratory, NASA/Goddard Space Flight Center, Greenbelt, MD, USA, where she conducts research in soil moisture retrieval and land surface hydrology, primarily through microwave remote sensing techniques.

Dara Entekhabi (M'04–SM'09–F'15) received the B.S. and M.S. degrees from Clark University, Worcester, MA, USA, and the Ph.D. degree from the Massachusetts Institute of Technology (MIT), Cambridge, MA, in 1990. He is currently a Professor with the MIT Department of Civil and Environmental Engineering. He is the Science Team Lead for the National Aeronautics and Space Administration's Soil Moisture Active and Passive mission that was launched on January 31, 2015. His research interests include terrestrial remote sensing, data assimilation, and coupled land–atmosphere systems modeling. Dr. Entekhabi is a Fellow of the American Meteorological Society and the American Geophysical Union.

Mahta Moghaddam (S'86–M'87–SM'02–F'09) received the B.S. degree (with highest distinction) from the University of Kansas, Lawrence, KS, USA, in 1986 and the M.S. and Ph.D. degrees in electrical and computer engineering from the University of Illinois at Urbana–Champaign, Champaign, IL, USA, in 1989 and 1991, respectively. She is a Professor of electrical engineering with the University of Southern California, Los Angeles, CA, USA. From 1991 to 2003, she was with the Radar Science and Engineering Section, NASA Jet Propulsion Laboratory, and from 2003 to 2011, she was a Professor of electrical engineering and computer science with the University of Michigan, Ann Arbor, MI, USA. She was a Systems Engineer for the Cassini Radar, the JPL Science Group Lead for the LightSAR project, and the Science Chair of the JPL Team X (Advanced Mission Studies Team). She is a member of the NASA Soil Moisture Active and Passive (SMAP) mission Science Team, a member of the NASA Advisory Council Earth Science Subcommittee, and the Principal Investigator of the AirMOSS Earth Ventures 1 mission. She has introduced new approaches for quantitative interpretation of multichannel radar imagery based on analytical inverse scattering techniques applied to complex and random media. Her most recent research interests include the development of new radar instrument and measurement technologies for subsurface and subcanopy characterization, development of forward and inverse scattering techniques of layered random media, and transforming concepts of radar remote sensing to near-field and medical imagining and therapy systems. Dr. Moghaddam is the Editor-in-Chief of the IEEE Antennas and Propagation Magazine.